Bartholomeeusen, G. *et al.* (2002). *Géotechnique* **52**, No. 9, 639–648

Sidere: numerical prediction of large-strain consolidation

G. BARTHOLOMEEUSEN*, G. C. SILLS*, D. ZNIDARČIĆ †, W. VAN KESTEREN‡, L. M. MERCKELBACH‡, R. PYKE§, W. D. CARRIER III¶, H. LIN**, D. PENUMADU**, H. WINTERWERP††, S. MASALA‡‡ and D. CHAN‡‡

Large-strain consolidation theory is widely used for the management of dredged disposal sites. The theory is universally accepted to deal with this problem, though the determination of the material properties is not yet standardised. Decisions made on this level can lead to the prediction of a totally different consolidation history. This paper describes the results of a prediction exercise, performed using a batch of sediment from the river Schelde (Antwerpen, Belgium). Numerical modellers were given the data of four calibration experiments and were then asked to predict another experiment. Settling column experiments (0·2–0·6 m in height) with density and pore pressure measurements provided the basis for the calibration data. The prediction demonstrated the significance of the soil compressibility at low effective stresses, when time-dependent behaviour is observed.

KEYWORDS: consolidation; numerical modelling

La théorie de la consolidation des grandes déformations est largement utilisé au niveau de la gestion des sites de residus dragués. En dépit d'une reconnaissance universelle de son efficacité dans ce domaine, il nous faut constater que cette théorie n'a jamais fait l'objet d'une standardisation de ses propriétés matérielles. Les décisions prises à ce niveau peuvent donner lieu à la prédiction d'un historique de la consolidation totalement différent. Cet article décrit les résultats d'un exercice de prédiction effectué à partir d'un lot de sédiments de la rivière Schelde (Anvers, Belgique). Les données de quatre expériences de calibrage ont été communiqués à des modeleurs numériques, afin que ceux-ci produisent des prédictions d'une autre expérience. Les donnés des expériences de calibrage provenaient des colonnes de tassement (d'une hauteur comprise entre 0·2 et 0·6 m) incorporant les mesures de densité et de contrainte de l'eau. La prédiction a démontré l'importance de la compressibilité des sols à basse contrainte effective, lorsque une dépendance au temps se manifeste.

INTRODUCTION

Goal and framework of the prediction exercise

When a soil–water mixture is deposited at a low initial density, a significant amount of deformation or surface settlement occurs. This situation was modelled by Gibson *et al.* (1981), using a continuum theory describing large-strain consolidation of a soil layer under its own weight. The theory consists of the continuity equations for the fluid and solid phase, momentum balance, Darcy–Gersevanov's flow relationship, and the assumption of the validity of the effective stress. A solution of the equations requires knowledge of material properties for deformation and flow. Both properties are assumed to be monotonic functions relating density or void ratio to the effective stress and permeability. Since Gibson's publication, experimental and numerical issues of large-strain consolidation have been reported in numerous papers: see for example Znidarčić *et al.* (1984), Tan *et al.* (1990), De Boer *et al.* (1996), Sills (1998) and Toorman (1999).

The numerical prediction of a physical process involves three parts: a relevant theory describing the physical phenomena, a suitable solution method, and the identification of appropriate material properties. The first two parts involve physics and mathematics, whereas the third part requires testing and expertise. Townsend & McVay (1990) reported the results of a numerical exercise that excluded the third aspect, in that participants were given the material functions and the initial conditions of a couple of test cases and were asked to predict the surface settlement and density profiles as a function of time. The general outcome of the exercise showed a good agreement between the results, which was expected as, with the material properties given, only numerical solution techniques were compared. Been & Sills (1981) published a similar set of experiments and produced numerical predictions based on back-analysis of the observed behaviour. This paper describes another large-strain consolidation exercise, but this time the focus was on the decision-making necessary to model experimental results, so that decisions had to be made about the appropriate form of the material functions.

Experiments were carried out in which a slurry of soil was introduced into a settling column and allowed to consolidate under its own weight. Measurements of density and pore water pressure were made. The results of four calibration experiments were provided, and participants were asked to predict the results of a fifth experiment for which only the initial condition was known. In this way the quality of models, theory and expertise could be evaluated together. These Class A predictions were compared with each other and with the results of the experiment at a seminar, named Sidere, held in Oxford on 25 September 2000.

Soil and experimental set-ups

Soil classification. The goal of Sidere was to perform this exercise on a natural soil that could be part of a dredging project or disposal operation. Many harbours around the world need maintenance dredging to ensure access for sea- and ocean-going vessels. As an example of the need to

Manuscript received 3 December 2001; revised manuscript accepted 16 June 2002.
Discussion on this paper closes 1 May 2003, for further details see p. ii.

* University of Oxford, UK.
† University of Colorado, USA.
‡ WL-Delft Hydraulics, The Netherlands.
§ Lafayette, California, USA.
¶ Argila Enterprises Inc., Lakeland, Florida, USA.
** University of Tennessee, USA.
†† Delft University of Technology, The Netherlands.
‡‡ University of Alberta, Canada.

predict settlement in a disposal site, the Slufter in the The Netherlands has been used to store dredged material from the Euro-port. The soil for the Sidere exercise was collected at low tide from the river Schelde in Antwerpen, Belgium. A single batch for the whole exercise was taken from a localised area to minimise field variation in the soil properties. The soil has a liquid limit of 39%, a plastic limit of 28% and a specific gravity of 2·72. Grain size distributions were performed with a laser diffraction technique, and the d_{10}, d_{50}, d_{90} sizes are 6, 70 and 210 μm respectively. On the plasticity chart the soil lies just beneath the A-line and is therefore classified as a silt of intermediate plasticity.

Experimental set-up. The calibration and prediction experiments were performed in settling columns using a standard methodology (Sills, 1995). The acrylic settling columns have an internal diameter of 102 mm and external diameter of 108 mm. Pore water pressure ports are located in the column at intervals of approximately 2 cm near the base and a larger spacing further up the column. The ports connect through a porous saturated material to a tube leading to a measuring unit that contains a pressure transducer, which can be linked in turn to the different ports. Density is measured non-destructively using an X-ray system originally developed by Been (1981). X-rays from a highly collimated beam are passed through the settling column and received in a detector assembly as a count rate, which can be converted to density by calibration. The X-ray assembly, source tube and detector are mounted on an arm driven by a stepper motor to traverse up and down the settling column. The accuracy of the system is better than ±0·01 kPa for pore pressure, ±2 kg/m^3 for density and ±1 mm for spatial resolution.

CALIBRATION EXPERIMENTS

Initial conditions

The aim of the calibration experiments was to provide the modellers with information that they would have to interpret. The initial densities were all greater than the structural density, the value that marks the transition from a fluid-supported suspension to a soil in which effective stresses exist (Sills, 1998). This ensured that the soil could be modelled as a continuum. Initial heights were chosen in the range 0·2–0·6 m. For these heights the experiments were relatively short in duration, but the effective stress still developed sufficiently to observe a clear range. Table 1 lists the initial conditions. It can be seen that the initial densities of the experiments Sidc2 and Sidc3 are a little higher than that of the prediction experiment Sidp1, while that of Sidc6 is a little lower. Experiment Sidc5 was started at a significantly lower density than Sidp1. The initial densities of Sidc2, Sidc3 and Sidc6 are relatively close to that of Sidp1. The initial height of experiments Sidc2 and Sidc5 is approximately one-third that of Sidc3, Sidc6 and Sidp1.

Self-weight consolidation behaviour

In this section a general explanation of large-strain consolidation is given. Consolidation is a time-dependent process, and two good observation measures are density and excess pore water pressure, u_e—that is the value above hydrostatic pressure.

During consolidation the sediment interface drops and an overlying layer of water is formed. These experiments are allowed to consolidate by self-weight only, so that at the base the solids' velocity is zero and the excess pore water pressure gradient, $\partial u_e/\partial x$, equals zero. Water flows upwards, causing a reduction in the excess pore water pressure and a corresponding increase in the effective stress and also in the density. Consolidation will continue until all the excess pore pressure has dissipated and the soil skeleton is entirely self-supported.

Figure 1 shows the density profiles for Sidc2. It can be seen that the density increases quickly during the first day, with further increases to 14 days. Fig. 2 shows the corresponding excess pore pressure data points, showing a triangular initial shape. The slope is equal to the initial buoyant density, defined as the slurry density minus the density of water. The excess pore pressures have dropped to zero by 14 days, demonstrating that consolidation is complete by this stage. The corresponding results for the other calibration experiments Sidc3, Sidc5, Sidc6 are shown in Figs 3–8. Owing to its larger initial height, the consolidation of Sidc3 takes longer than Sidc2, so that the 1 day density profile, shown in Fig. 3, represents an earlier stage in the consolidation process. An increase in density can clearly be seen, working its way up from the bottom of the

Table 1. Initial conditions of Sidere experiments

Experiment	h_{init} [m]	ρ_{init} [kg/m^3]
Sidc2	0·215	1542
Sidc3	0·570	1556
Sidc5	0·213	1314
Sidc6	0·592	1486
Sidp1	0·565	1495

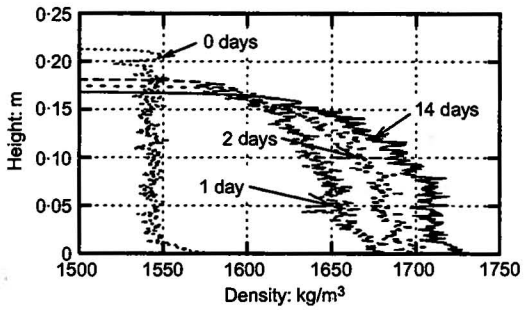

Fig. 1. Density profiles, Sidc2

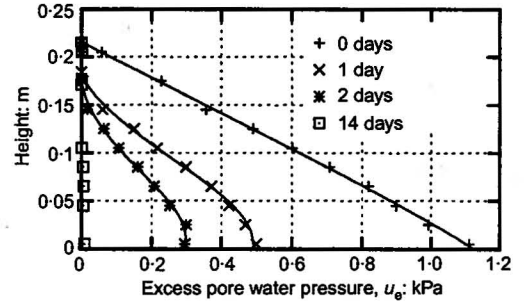

Fig. 2. Excess pore water pressure, Sidc2, with curve fit

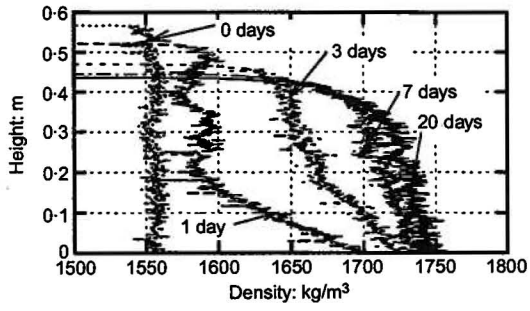

Fig. 3. Density profiles, Sidc3

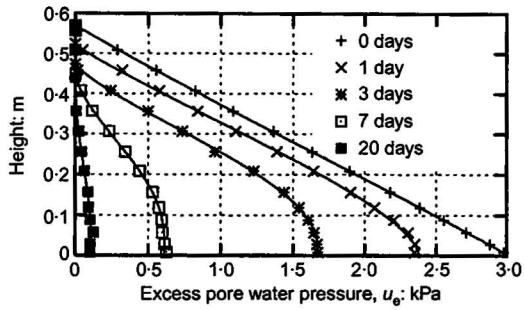

Fig. 4. Excess pore water pressure, Sidc3, with curve fit

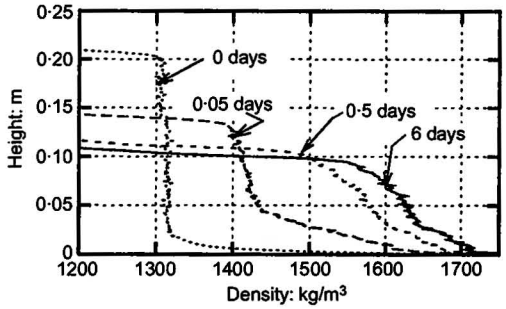

Fig. 5. Density profiles, Sidc5

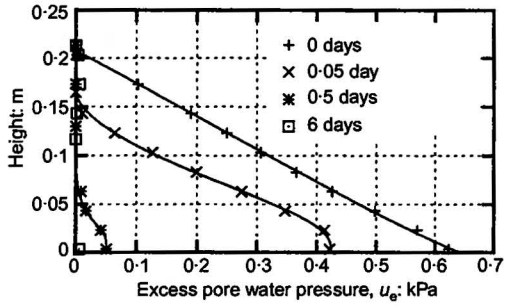

Fig. 6. Excess pore water pressure, Sidc5, with curve fit

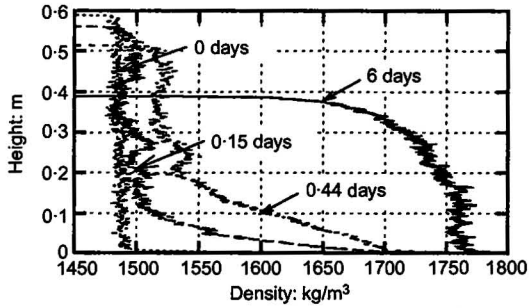

Fig. 7. Density profiles, Sidc6

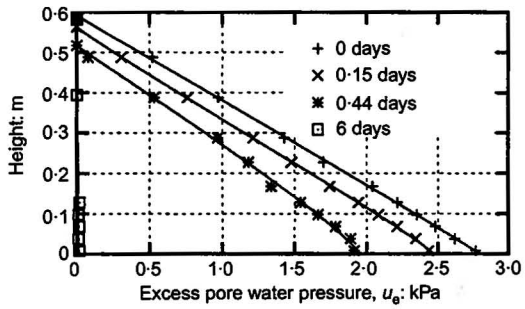

Fig. 8. Excess pore water pressure, Sidc6, with curve fit

column, having reached 0·2 m in the 1 day profile. The same feature can be seen in Fig. 5 for Sidc5, at 0·05 m on 0·05 days and in Fig. 7 at 0·1 m and 0·2 m for 0·15 and 0·44 days respectively for Sidc6.

Material functions

Compressibility. This is characterised through a correlation between void ratio and effective stress. The void ratio is calculated immediately from the density profiles, and the integration of the density profile yields the vertical total stress, σ. At the levels at which the pore water pressure, u_w, is measured, the vertical effective stress can then be calculated as $\sigma' = \sigma - u_w$.

Figure 9 depicts an overview of the compressibility data calculated from the calibration experiments Sidc2, Sidc3, Sidc5 and Sidc6. For effective stress values greater than ~0·6 kPa a unique relationship is visible, whereas for stresses below this value the data points cover a triangular-shaped area. The accuracy for the calculation of effective stress is ±0·02 kPa, so the observed spread is not due to experimental error. A good prediction will therefore depend significantly on the assumptions made in this area, particularly in the early stages while the effective stresses are low.

Permeability. A relationship is sought between permeability and void ratio. Gibson assumed Darcian flow in soil with the solids moving relative to the water (Darcy, 1856; Gersevanov, 1934):

$$-\frac{e}{(1+e)}(v_f - v_s) = k\frac{1}{\rho_f g}\frac{\partial u_e}{\partial x} \tag{1}$$

where v_f and v_s are the velocity of fluid and solids respectively. In the case of an undrained bottom boundary, the left-hand term of equation (1) reduces to the solids velocity, v_s. Material coordinates 0·1, 0·2, ..., 0·9 are defined as corresponding to 10%, 20%, ..., 90% of the solids, beneath the surface and the solids velocity is calculated from the heights of these coordinates in consecutive density profiles. Subsequently, the solids velocity is approximated by a central difference approximation.

In order to calculate the excess pore water pressure gradient, a smoothed curve is fitted through the profiles of excess pore pressure plotted against height. The function has to fulfil the following three conditions: excess pore water pressure at the sediment surface has to be zero; at the bottom the boundary condition, $(\partial u_e/\partial x)_{x=0} = 0$, has to be satisfied; and in between the expression has to be flexible enough to fit the data points well. A curve fit of the Weibull function (Weibull, 1951) is chosen:

$$u_e = m[1 - \exp(ax^b)] \tag{2}$$

with m, a and b determined by a Nelder–Mead minimisation or simplex method. As can be seen in Figs 2, 4, 6 and 8, the fitted curve Δ, shown as a solid line, passes close to all the individual data points. The correlation between permeability and void ratio obtained from the use of equation (1) is shown in Fig. 10.

NUMERICAL PREDICTIONS

The particular approach adopted by Gibson *et al.* (1981) was to solve the equations of continuity and flow using material or Lagrangian coordinates, z, without restriction to small strains and with the inclusion of the effects of self-weight. The governing equation can be written in terms of void ratio, e, as

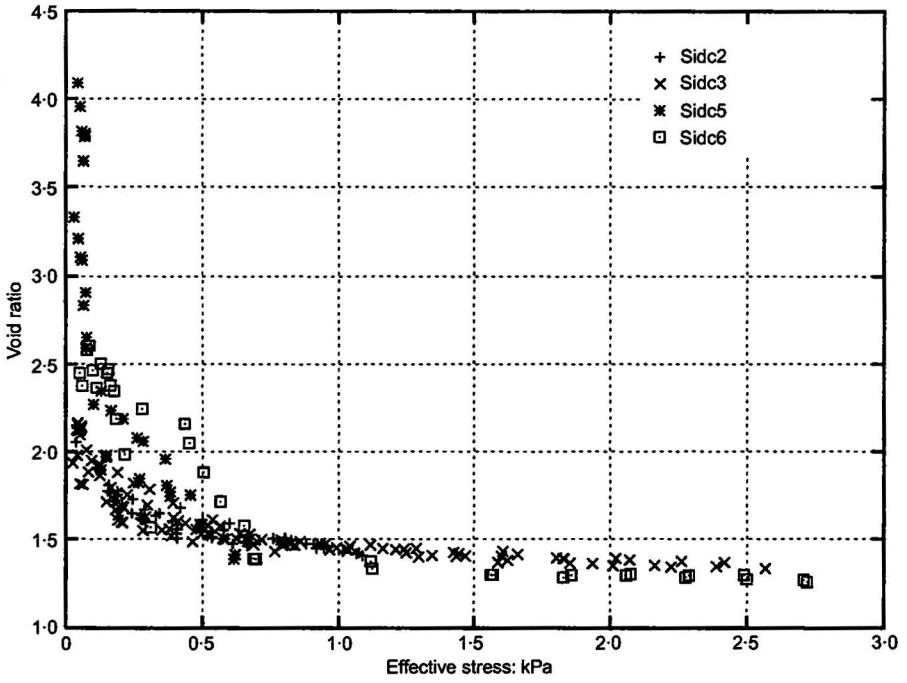

Fig. 9. Overview of the compressibility data of the calibration experiments (Sidc2, Sidc3, Sidc5, Sidc6)

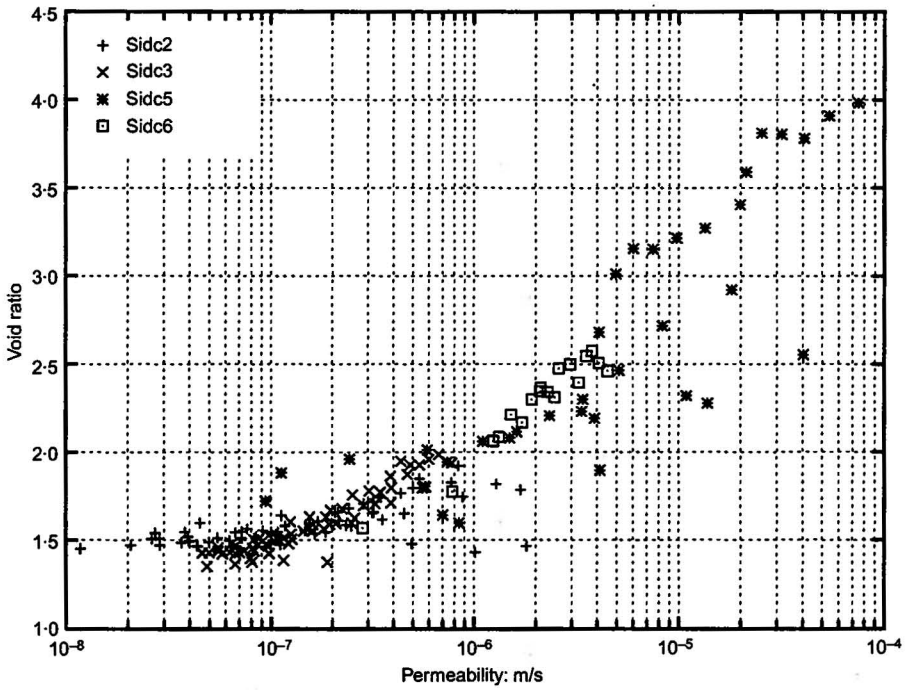

Fig. 10. Overview of the permeability data of the calibration experiments (Sidc2, Sidc3, Sidc5, Sidc6)

$$\left(\frac{\rho_s}{\rho_w}-1\right)\frac{d}{de}\left[\frac{k(e)}{1+e}\right]\frac{\partial e}{\partial z}+\frac{\partial}{\partial z}\left[\frac{k(e)}{\rho_w g(1+e)}\frac{d}{de}[\sigma'(e)]\frac{\partial e}{\partial z}\right] = -\frac{\partial e}{\partial t}; \quad (3)$$

It can be seen that there are two components on the left-hand side of the equation, the first having the form of the advection equation and the second the form of the diffusion equation. The second term represents the consolidation process due to a changing effective stress, and, for a physical problem in which settling under gravity dominates the behaviour, the first term is also significant. Various other authors have used the same approach, but have written the equation in terms of space or Eulerian coordinates with a moving boundary condition, or in terms of a different dependent variable. Analytical solutions can be found only under special conditions in which the coefficients of the equation are constant. For example, Gibson *et al.* (1981) solved equation (3) with a constant finite strain coefficient of consolidation,

$$g(e)=\frac{k(e)}{\rho_w}\frac{1}{1+e}\frac{d\sigma'}{de}$$

and a constant

$$\lambda(e) = -\frac{\mathrm{d}}{\mathrm{d}e}\frac{\mathrm{d}e}{\mathrm{d}\sigma'}$$

Lee & Sills (1979) wrote equation (3) without the advection term using Eulerian coordinates and solved the large-strain problem without self-weight assuming that the coefficient of consolidation, c_v as defined by Terzaghi, is constant. If it is assumed that, as well as the effect of self-weight being insignificant, strains are small and c_v is constant, then Terzaghi's small-strain equation of consolidation is recovered.

The governing equation may be solved numerically so that more realistic assumptions may be made about the values of soil parameters and the constraints of the boundaries. In particular, permeability and compressibility can be allowed to vary in any monotonic manner with void ratio. The numerical methods required to solve such equations are well defined, with the finite difference technique being the most popular among the participants. The differences between predictions then occur either as a result of decisions made to simplify the governing equations, by differences in the functions chosen to model the parameter relationships, or by the use of different iterative methods to satisfy the boundary conditions. Figs 9 and 10 show some variation in the compressibility and permeability correlations. The use of a simple function to represent these relationships requires the choice of the criteria for best fit. A further complication for the compressibility relation was the incorporation of the initial condition, given that the prediction experiment had an initial void ratio of 2·52, which was lower than the initial values of some of the calibration experiments. Table 2 provides information about the models and parameter relationships used by each of the participants. The choices made by the participants were influenced by their previous experiences and main areas of interest. All the participants had been offered sediment to enable them to carry out their own testing in addition to the results provided by Oxford, but Znidarčić was the only one to undertake this. On the basis of his results, he reduced the compressibility of his soil, leading to the closest prediction over the first 7 days but the largest final bed thickness. Winterwerp's model assumed that the sediment existed initially in suspension, and he assumed sedimentation before consolidation. Merckelbach's model incorporates the possibility of segregation. All the participants except Sills and Pyke used the Gibson large-strain equations as the basis for their numerical models of the consolidation process. Sills used an analytical solution to the Terzaghi small strain equations to predict the dissipation of excess pore pressures, taking the best-fit value of c_v from the calibration experiments. The final density profile was calculated from the compressibility correlation, and the intermediate profiles were calculated from the total stress and the excess pore pressures, adjusting the soil layer thickness in order to maintain a constant mass balance. Pyke's prediction was based directly on the Terzaghi small-strain solution with the bed thickness continuously updated as consolidation proceeded.

The participants were asked to predict the surface settlement curves, with an output at specified times. Fig. 11 shows the results of these predictions along with the experimental observations. It is immediately apparent that all the solutions show too fast a consolidation process, with the majority of the settlement complete after 7 days. The experimental result, on the other hand, suggests that settlement is still ongoing at 7 days. Comparing the predictions with the measurement at 0·8, 1·2 and 5·9 days, there is a 10–15% difference. After 7 days the surface has settled by 20% of the original bed thickness, and the average difference between the predictions and actual bed thickness is 7%. A later measurement at 15 days showed that the excess pore pressures had virtually dissipated and settlement had ceased. By this time, the bed thickness had dropped from the original value of 0·565 m to 0·410 m, and the majority of the predictions are within 5% of the true value. In engineering terms, therefore, all of the predictions were good. The differences that existed can generally be attributed to differences in the model and the functional relationships. Thus Winterwerp's decision to treat the initial density as identifying a suspension led to a very fast initial collapse to a soil

Table 2. Details of numerical programs of the participants (units in kPa and m/s unless noted otherwise).

Participants	Dependent variable	Parameter choice
Bartholomeeusen	Void ratio	$e = -1{\cdot}07\ \sigma'^{0{\cdot}14} + 2{\cdot}52$ $e = 0{\cdot}27\ln(k) + 5{\cdot}95$
Carrier (Carrier III *et al.*, 1983)	Void ratio	$e = 2{\cdot}933[\mathrm{Pa}]\ (\sigma' + 5{\cdot}32)^{-0{\cdot}10}$ $k = \frac{8{\cdot}96 \times 10^{-9} e^{8{\cdot}08}}{1+e}$
Lin & Penumadu	Void ratio	$e = -0{\cdot}22\ln(\sigma') + 1{\cdot}46$ $k = 0{\cdot}0072\ e^{6{\cdot}75}$
Masala & Chan	Void ratio	$e = 2{\cdot}81[\mathrm{Pa}^{-1}]\ \sigma'^{-0{\cdot}102}$ $k = 1{\cdot}38 \times 10^{-3}\ \mathrm{m/day}\ e^{5{\cdot}75}$
Merckelbach (Merckelbach, 2000)	Solids vol. fraction, Φ $\Phi = \frac{\phi_{\mathrm{fines}}}{1-\phi_{\mathrm{sand}}}$	$\sigma' = 3 \times 10^{13}\ \Phi^{-14{\cdot}3}$ $k = 2 \times 10^{-19}\ \Phi^{14{\cdot}3}$ (26% fines)
Pyke	Void ratio	Linear interpolation for k(e) and $\sigma'(e)$ from a table
Sills	Excess pore pressure	$\sigma' \leqslant 0{\cdot}2$ $e = -0{\cdot}21\ln(\sigma') + 1{\cdot}26$ $\sigma' > 0{\cdot}2$ $e = -0{\cdot}11\ln(\sigma') + 1{\cdot}42$ $c_v = 3 \times 10^{-7}\ \mathrm{m^2/s}$
Van Kesteren (Van Kessel & Van Kesteren, 2002)	Void ratio	$\sigma' = \exp(11{\cdot}27 - 8{\cdot}0\ e)$ $k = \exp(-21{\cdot}55 + 3{\cdot}6\ e)$
Winterwerp (Winterwerp, 1999)	Solids vol. fraction Φ	$\sigma' = 6 \times 10^{-6}\ \Phi^{-19}$ $k = 1{\cdot}6 \times 10^{-10}\ \Phi^{19}$
Znidarčić (Yao *et al.*, 2002)	Void ratio	$e = 1{\cdot}69\ (\sigma' + 0{\cdot}046)^{-0{\cdot}12}$ $k = 4{\cdot}14 \times 10^{-9} e^{6{\cdot}59}$

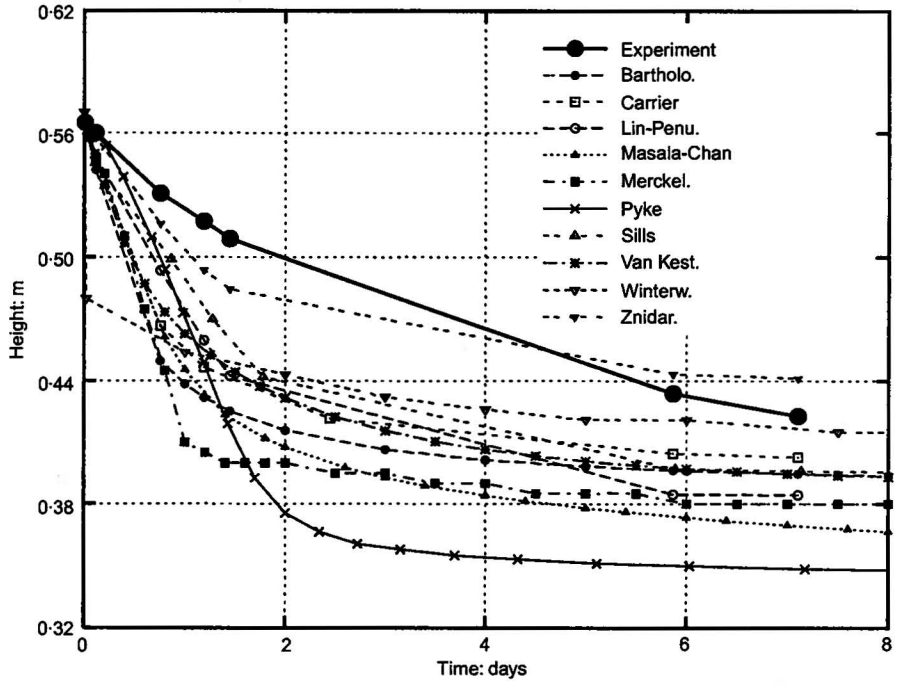

Fig. 11. Comparison of experimental and predicted settlement curves, Sidp1

state. Thereafter his predicted settlement became increasingly close to the experimental observation, so that after 7 days it was the best estimate. Pyke's choice of compressibility using the lower bound of the void ratio–effective stress correlation led to a smaller predicted bed height than any other from 1·5 days onwards.

The second specified prediction was of the density profile as a function of height after 7 days, as shown in Fig. 12. As would be expected from the surface settlement predictions, all except Znidarčić show the density to be greater than the measured values. The shapes of the profiles are generally similar, with the largest differences occurring at the low effective stress levels near the top of the bed. This is not surprising, since this is the region where small differences in the choice of compressibility relationships will be most apparent. This is most clearly visible in Winterwerp's solution, which was unique in its modelling of a suspension phase before the start of consolidation.

DISCUSSION

It can be concluded from the previous section that the later stages of the consolidation process can be predicted reasonably well. The rate of consolidation in the early stage is generally predicted to occur too fast. This section examines possible explanations for this discrepancy.

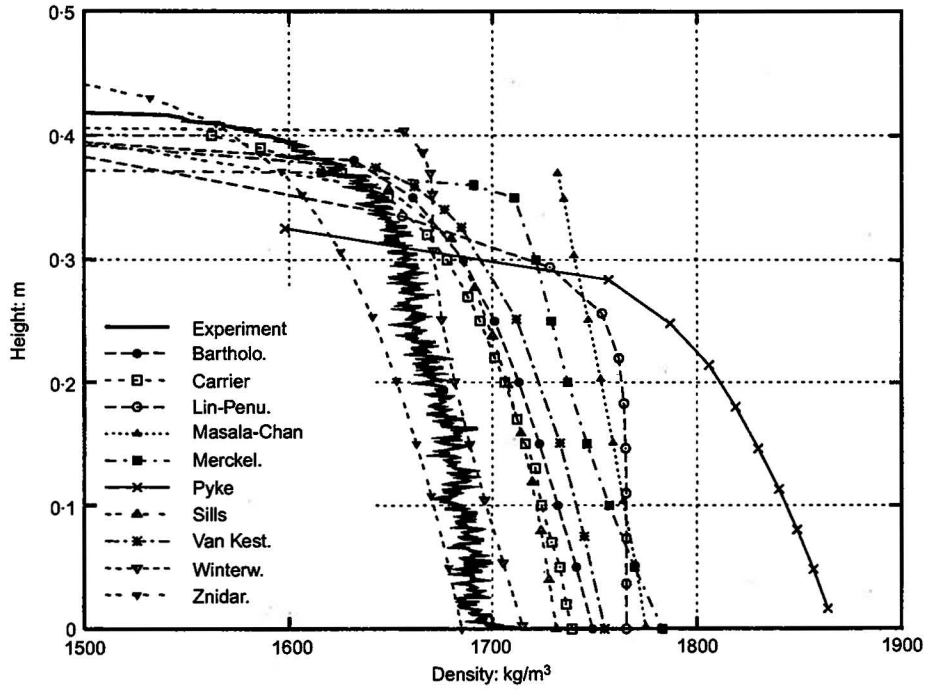

Fig. 12. Comparison of experimental and predicted density profiles, Sidp1

Material

The results from the calibration experiments can be expected to apply to the prediction exercise only if the soil is essentially the same in all the experiments. This was assessed in two ways, the first by measuring the particle sizes at different locations in a selection of the columns and the second by comparing the parameter relationships of compressibility and permeability. A grain size analysis was performed on experiments Sidc3, Sidc6 and Sidp1. Samples were taken at different heights in the column at approximately 50 mm, 100 mm, 200 mm and 300 mm above the base. The coarser material, larger than 300 μm, has been sieved, and the smaller sizes have been determined with a laser diffraction technique. Fig. 13 depicts bands defining the extreme values of all the samples. As can be seen the bands are very close, demonstrating that particle segregation did not occur in any of the experiments.

Figure 14 shows the compressibility data of Sidp1 compared with the calibration data set presented earlier in Fig. 9. For effective stresses smaller than ~0·6 kPa, the Sidp1 results lie well within the trend. Above this value the data of the prediction experiment lie just above the trend, but the difference is of the same order as observed in Fig. 9 between Sidc3 and Sidc6. The settlement curve predictions (Fig. 11) showed a difference of approximately 5% from the measured value for the final stages of the consolidation. The observed difference in the compressibility data is therefore consistent with the experimental data and model prediction. The permeability for void ratios smaller than 2 is absolutely within the trend, as presented in Fig. 15. A spread of just less than an order of magnitude is observed for the higher void ratios, but a similar spread was evident also for the calibration data. Both material properties of the prediction experiment are therefore within the range of the calibration

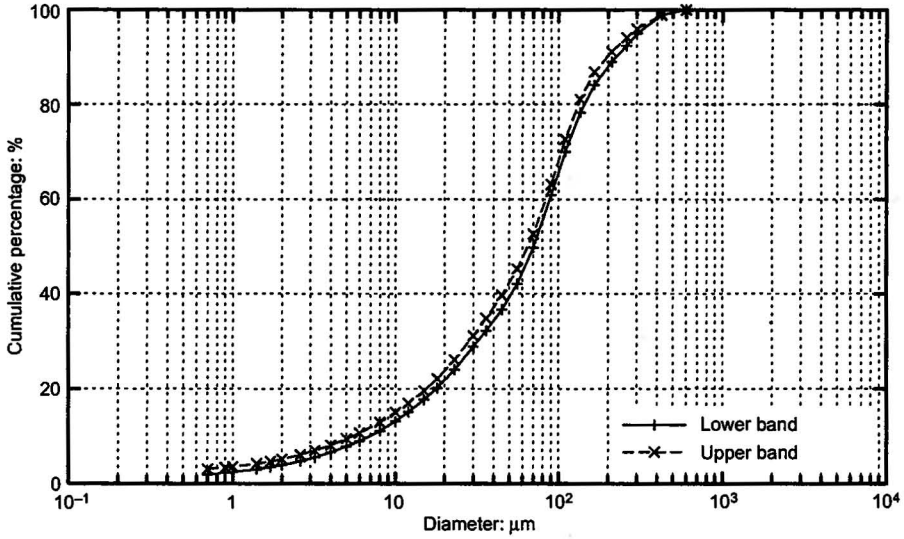

Fig. 13. Grain size distributions: experiments Sidc3, Sidc6, Sidp1 and two original samples

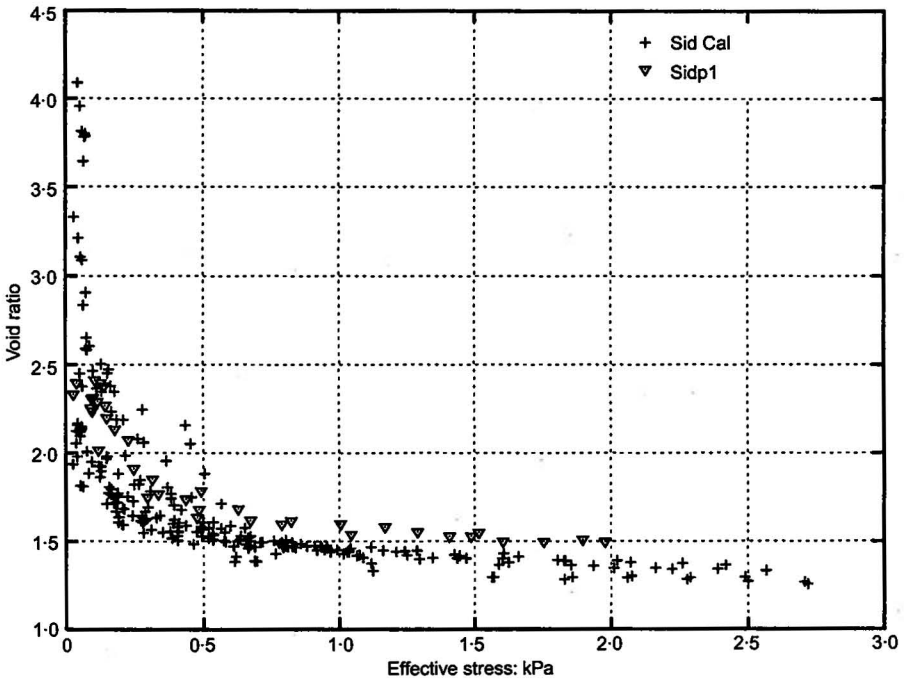

Fig. 14. Effective stress – void ratio data experiment Sidp1 compared with calibration data

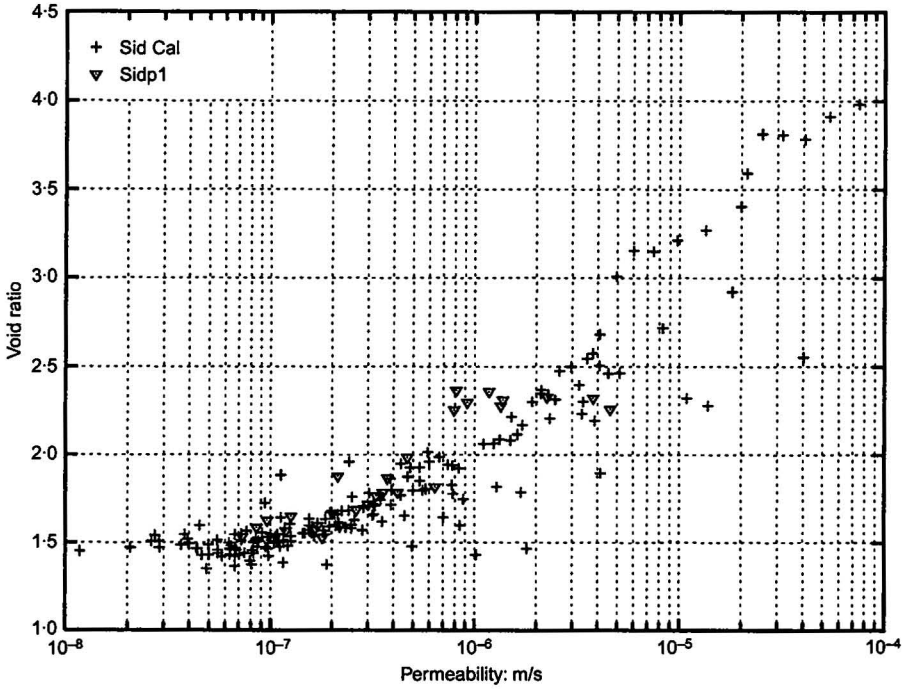

Fig. 15. Permeability – void ratio data experiment Sidp1 compared with calibration data

experiments, so that the discrepancy between the predictions and the experimental results should therefore be sought on the level of the theoretical assumptions.

Time dependence

For small-strain consolidation behaviour Leroueil *et al.* (1985) have pointed out that the rheological model for compressibility consisting of a function $R(e, \sigma')$ is not appropriate to describe the compressibility behaviour of a soil. Suggestions have been made for rheological models incorporating rate effects, for instance $R(e, \sigma', \partial e/\partial t)$ or $R(e, \sigma', \partial e/\partial t, \partial \sigma'/\partial t)$. Been & Sills (1981) addressed this time dependence by the use of an imaginary layer of soil above the actual bed. The consolidation of the combined thickness was modelled using the Gibson large-strain equations combined with various assumptions of linearity. Although it proved possible to simulate the observed behaviour well, this approach does not address the mechanism of the time dependence and has therefore not been pursued.

In order to investigate this matter, Sidc3 is analysed in more detail. Fig. 16 shows the correlation of void ratio with effective stress with time. It is clear that the relationships have a downward trend with time, especially for effective stresses smaller than ~0·6 kPa. Subsequently, from the individual profiles average void ratios are calculated around

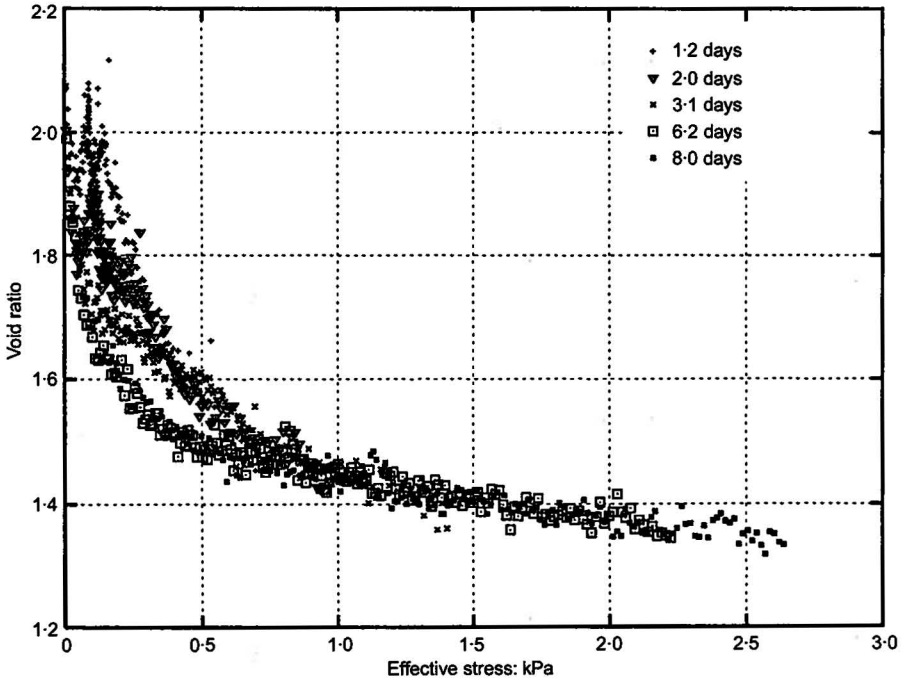

Fig. 16. Effective stress – void ratio data experiment Sidc3

four fixed effective stress levels: 0·1, 0·4, 1·2 and 2·3 kPa (±0·01 kPa). These average void ratios are plotted in time, as shown in Fig. 17. A decrease in void ratio is clearly observed for the smaller effective stresses. For instance, the decrease in void ratio for the 0·1 kPa level is about 15%, and 7% for the 0·4 kPa level, whereas the change is smaller than 2% for the 1·2 kPa level and constant for the 2·3 kPa level. Previously similar trends for natural soils have been observed in settling column experiments reported by Sills (1995).

A numerical model that does not include this inherent time dependence must use a constant relationship. Assuming that it is calibrated to the lower bound of the compressibility, the error on the void ratio at an early stage lies in the range 7–15% for effective stresses between 0·1 and 0·4 kPa. In the previous section the average error of the surface settlement in the early stages ranged from 10% to 15%. The observed trend of Fig. 16 shows that a given effective stress will correspond to a higher void ratio in the early stages of consolidation and a lower one later on. If the lower correlation between effective stress and void ratio is chosen, this will lead inevitably to a faster predicted settlement rate.

CONCLUSIONS

In predicting settlement and consolidation due to self-weight, the first decision to be made is whether or not to include both suspension and consolidation processes. In a situation such as that tested in the laboratory or occurring in disposal sites, where the initial condition is one of equal total stress and pore pressure so that the effective stress is zero, this can be an important decision. The diffusion part of the Gibson equation is valid only when effective stresses exist. The inclusion of this term, or variants of it, in the governing equation therefore implies that consolidation is occurring as a result of immediate increases in the effective stresses. Winterwerp was the only participant to depart significantly from this assumption, in his inclusion of a suspension stage that collapsed very quickly at the start of his prediction.

This exercise has identified both strengths and weaknesses in the current understanding of soft soil consolidation. In terms of being able to predict the final thickness of the consolidated bed, all the participants achieved an accuracy acceptable for application to field problems. It is clear that, in practice, consultants can be very successful in predicting field behaviour where they have experience of similar soils and conditions. However, this exercise has highlighted some aspects of behaviour that cannot be easily predicted and which may have serious implications in particular situations. The overestimate of the initial settling rate common to all the predictions has been shown to be due to an inherent time- or rate-dependence of the correlation between effective stress and void ratio. On the laboratory scale of the settling column experiments, this was most marked at effective stress levels lower than 1 kPa and times up to about 3 days. If the same time period operated in the field also, it would not be particularly significant in terms of predicting the consolidation of soil in a deep slurry disposal site. However, it is more likely that it is the low stress level that is associated with this time-dependent process, and the effective stresses could stay low for a long time through a deep bed, such as the 30 m deep Slufter site in the Netherlands and the 10 m deep underwater disposal sites in Antwerpen, Belgium. Neglecting this effect could therefore significantly overestimate the storage capacity in the shorter term. In practice, an upper bound on the bed height can be obtained by choosing the earliest values of the effective stress void ratio correlation, with the later values used to provide a long-term solution.

The prediction seminar has highlighted a complex compressibility behaviour for low effective stresses, in which the choice of the compressibility relationship plays an important role as well as the stress history (initial density), and above all a significant time-dependent phenomenon has been observed. An incorporation of these phenomena in large-strain consolidation theory would lead to better predictions.

ACKNOWLEDGEMENTS

Financial support from Dredging International and the Engineering and Physical Science Research Council, UK, is

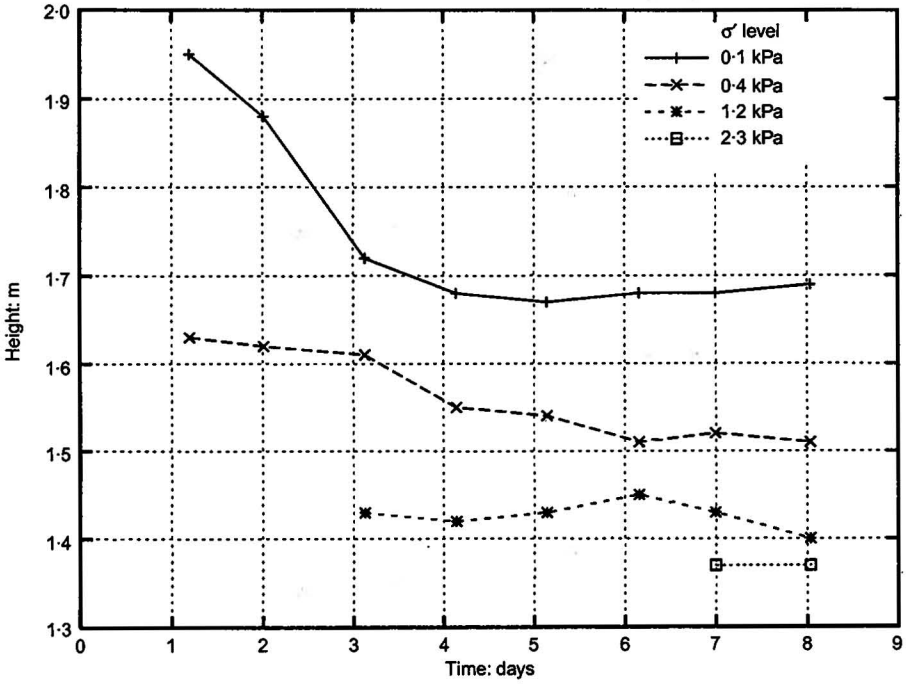

Fig. 17. Change in void ratio for constant effective stress levels, Sidc3

gratefully acknowledged, as is the development of the experimental set-up by Mr Ken Howson and Mr Chris Waddup.

We are particularly pleased that Professor Bob Gibson was able to attend the Sidere seminar as an honorary guest.

REFERENCES

Been, K. (1981). Non-destructive soil bulk density measurement using x-ray attenuation. *Geotechnical Testing J.* pp. 169–176.

Been, K. & Sills, G. C. (1981). Self-weight consolidation of soft soils. *Géotechnique* **31**, 519–535.

Carrier III, W. D., Bromwel, L. G. & Somogyi, F. (1983). Design capacity of slurried mineral waste ponds. *J. Geotechn. Engng* **109**, No. 5, 699–716.

Darcy, H. P. G. (1856). *Les fontaines publiques de la ville de Dijon.* Paris: Dalmont.

De Boer, R., Schiffman, R. L. & Gibson, R. E. (1996). The origins of the theory of consolidation: the Terzaghi–Fillunger dispute. *Géotechnique* **46**, No. 2, 175–186.

Gersevanov, N. M. (1934). Dinamika mekhaniki gruntov. *Grosstroiisdat* **2**.

Gibson, R. E., Schiffman, R. L. & Cargill, K. W. (1981). The theory of one-dimensional consolidation of saturated clays. 2. Finite non-linear consolidation of thick homogeneous layers. *Can. Geotech. J.* **18**, 280–293.

Lee, K. & Sills, G. C. (1979). A moving boundary approach to large strain consolidation of thin soil layer. *Proc. 3rd Int. Conf. Numer. Methods Geomech.*, Aachen, Germany, 163–173.

Leroueil, S., Kabbaj, M., Tavenas, F. & Bouchard, R. (1985). Stress–strain–strain rate relation for the compressibility of sensitive natural clays. *Géotechnique* **35**, No. 2, 159–180.

Merckelbach, L. M. (2000). *Consolidation and strength evolution of soft mud layers.* PhD thesis, Delft University of Technology.

Sills, G. C. (1995). Time dependent processes in soil consolidation. *Proceedings of the international symposium on compression and consolidation of clayey soils*, (eds H. Yoshikuni and O. Kusakabe) pp. 875–890. Rotterdam: A. A. Balkema.

Sills, G. C. (1998). Development of structure in sedimenting soils. *Phil. Trans. Roy. Soc. Lond. A* **356**, 2515–2534.

Tan, T. S., Yong, K. Y., Leong, E. C. & Lee, S. L. (1990). Behaviour of clay slurry. *Soils Found.* **30**, No. 4, 105–118.

Toorman, E. A. (1999). Sedimentation and self-weight consolidation: constitutive equations and numerical modelling. *Géotechnique* **49**, No. 6, 709–726.

Townsend, F. C. & McVay, M. C. (1990). SOA: large-strain consolidation predictions. *J. Geotech. Engng* **116**, No. 2, 166–176.

Van Kessel, T. & Van Kesteren, W. G. M. (2002). Gas production and transport in artifical sludge depots. *Waste Management* **22**, 19–28.

Weibull, W. (1951). A statistical distribution function of wide applicability. *J. App. Mech.* **18**, No. 3, 293–297.

Winterwerp, J. C. (1999). *On the dynamics of high-concentrated mud suspensions.* PhD thesis, Delft University of Technology.

Yao, D. T. C., Oliveira-Filho, W. L., Cai, X. C. & Znidarčić, D. (2002). Numerical solution for consolidation and dessication of soft soils. *Int. J. Numer. Anal. Methods Geomech.* **26**, No. 2, 139–161.

Znidarčić, D., Croce, P., Pane, V., Ko, H., Olsen, H. W. & Schiffman, R. L. (1984). The theory of one-dimensional consolidation of saturated clays: 3. Existing testing procedures and analyses. *Geotech. Test. J.* **7**, No. 3, 123–134.